PROCEEDINGS A

rspa.royalsocietypublishing.org

Research

Cite this article: Scolan Y-M, Korobkin AA. 2015 Water entry of a body which moves in more than six degrees of freedom. *Proc. R. Soc. A* **471**: 20150058.
http://dx.doi.org/10.1098/rspa.2015.0058

Received: 28 January 2015
Accepted: 11 March 2015

Subject Areas:
ocean engineering

Keywords:
water impact, three-dimensional flow, free body motion, hydrodynamic loads

Author for correspondence:
Y.-M. Scolan
e-mail: yves-marie.scolan@ensta-bretagne.fr

Electronic supplementary material is available at http://dx.doi.org/10.1098/rspa.2015.0058 or via http://rspa.royalsocietypublishing.org.

THE ROYAL SOCIETY PUBLISHING

Water entry of a body which moves in more than six degrees of freedom

Y.-M. Scolan[1] and A. A. Korobkin[2]

[1]ENSTA Bretagne, LBMS, Brest, France
[2]School of Mathematics, University of East Anglia, Norwich NR4 7TJ, UK

The water entry of a three-dimensional smooth body into initially calm water is examined. The body can move freely in its 6 d.f. and may also change its shape over time. During the early stage of penetration, the shape of the body is approximated by a surface of double curvature and the radii of curvature may vary over time. Hydrodynamic loads are calculated by the Wagner theory. It is shown that the water entry problem with arbitrary kinematics of the body motion, can be reduced to the vertical entry problem with a modified vertical displacement of the body and an elliptic region of contact between the liquid and the body surface. Low pressure occurrence is determined; this occurrence can precede the appearance of cavitation effects. Hydrodynamic forces are analysed for a rigid ellipsoid entering the water with 3 d.f. Experimental results with an oblique impact of elliptic paraboloid confirm the theoretical findings. The theoretical developments are detailed in this paper, while an application of the model is described in electronic supplementary materials.

1. Introduction

We consider a three-dimensional object with a smooth surface, such as the bow part of a ship hull or the fuselage of an aircraft, approaching the water surface after lifting off or arriving from the atmosphere and penetrating the liquid-free surface. The body motion can be computed only by numerical means by taking into account the large displacements of the body, the cavity formation behind the body and the viscous forces acting on the body surface. This problem was studied by Kleefsman *et al.* [1], Maruzewski *et al.* [2], Tassin *et al.* [3], Yang & Qiu [4] among others. The early stage of water entry, when the wetted surface is in rapid expansion, is difficult to

capture numerically but this is the stage during which the hydrodynamic loads acting on the body are very high and may affect the body motions even for longer times.

We focus on the initial stage of the three-dimensional motion of a free body just after the time instant, $t = 0$, at which the body touches the water surface at a single point. We consider bodies whose dimensions are of the order of few metres, such as the fuselage of an aircraft or the bow part of a ship hull. For the water entry of such shapes the following assumptions are usually made: (i) the viscous effects are neglected as neither a boundary layer nor a separated flow has time enough to develop, (ii) the surface tension effects are not taken into account since the local curvature of the free surface is very small (except at the jet root), and (iii) the acceleration of the fluid particles exceeds the acceleration of gravity. These are the reasons for which neither Reynolds nor Froude and Weber numbers are included in the present problem.

In this analysis, the liquid is assumed to be incompressible and inviscid. The generated flow is irrotational and three-dimensional. Initially, $t = 0$, the water surface is flat and horizontal. The body surface in the contact region is approximated by a double curvature surface with two radii of curvature, R_x and R_y, which are not necessarily equal and may depend on time t.

Under the assumption of large curvature radii compared with the penetration depth, the resulting boundary-value problem is known as the Wagner entry problem [5] or 'flat-disc approximation' or Wagner's approach. This three-dimensional problem was studied in the past for the standard case of the vertical entry of an elliptic paraboloid [6–9]. Note that the Wagner theory assumes small deadrise angles and the wetted area, which expands in all directions over time. For more complex body motions, the oblique impact of an axisymmetric body was studied in Moore *et al.* [10] and the oblique impact of an elliptic paraboloid in Scolan & Korobkin [11] This paper aims at generalizing the entry of a smooth three-dimensional body that moves in all possible d.f. and also changes its shape over time. We are unaware of results by others dealing with such complex motions of the body entering water and the corresponding three-dimensional flows. It is shown in this paper that angular motions of a body change significantly the hydrodynamic loads and their distributions over the wetted part of the body surface. The pressure distribution is carefully analysed in §5, the zones of negative loads are identified, and the duration of the Wagner stage is examined.

The physical formulation of the entry problem within the Wagner approach is illustrated in figure 1. The jet flow originated at the periphery of the wetted part of the body surface is not shown in figure 1. The water-entry problem for an arbitrary smooth body is formulated in terms of the displacement potential [12,13] $\phi(x, y, z, t)$

$$\left.\begin{aligned} &\nabla^2\phi = 0 \quad (z < 0),\\ &\phi = 0 \quad (z = 0,\ (x, y) \notin D(t)),\\ &\phi_{,z} = f(x, y, t) \quad (z = 0,\ (x, y) \in D(t)),\\ &\phi \to 0 \quad (x^2 + y^2 + z^2 \to \infty)\\ \text{and}\quad &\phi \in C^2(z < 0) \cap C^1(z \le 0). \end{aligned}\right\} \tag{1.1}$$

Here the lower half-plane $z < 0$ corresponds to the flow domain, $D(t)$ is the contact region between the entering body and the liquid, the rest of the boundary, $z = 0$, $(x, y) \notin D(t)$, corresponds to the liquid-free surface. The position of the entering body surface is described by the equation $z = f(x, y, t)$. In this paper, the function $f(x, y, t)$ includes the 6 d.f. of the rigid body motions and the deformations of the body surface expressed in an earth-fixed coordinate system. The last condition in (1.1) implies that the displacement potential ϕ is a smooth function in the flow region and is continuous together with its first derivatives $\phi_{,x}$, $\phi_{,y}$ and $\phi_{,z}$ up to the boundary including the boundary [14]. The latter condition is equivalent to the Wagner condition [5] and serves to determine the shape and position of the contact region $D(t)$. Note that the time t is a parameter in this formulation. The problem can be solved at any time instant independently. The derivatives $\phi_{,x}$, $\phi_{,y}$ and $\phi_{,z}$ provide the displacements of liquid particles in the corresponding directions.

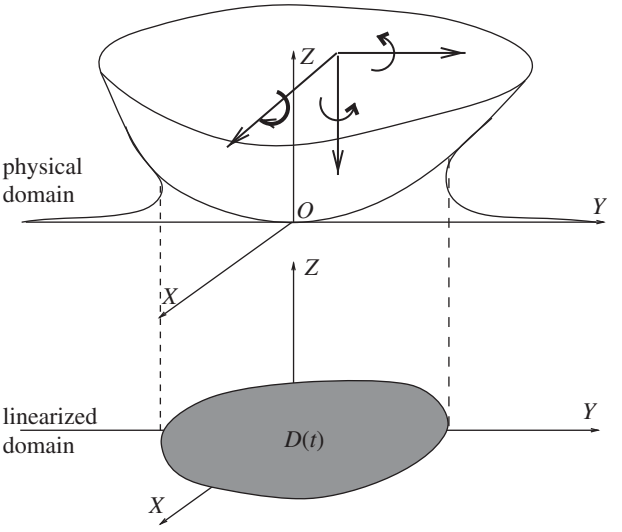

Figure 1. Sketch of a three-dimensional body entering an initially flat-free surface. The translational and rotational motions (thick arrows) are described in an earth-fixed coordinate system. In the linearized domain, $D(t)$ is the instantaneous expanding wetted surface. This is the projection of the actual wetted surface on the horizontal plane (x, y). The contact line is the intersection line between the moving body surface and the deformed free surface in both physical and linearized domain.

The function $f(x, y, t)$ from (1.1) is determined in §2 for the given motions of a rigid body. The displacement potential $\phi(x, y, 0, t)$ in the contact region $D(t)$ and the shape of this region are determined in §3. Hydrodynamic forces and moments acting on the body are calculated in §4. The hydrodynamic pressure distribution is analysed in §5. In §6, we consider the problem of a rigid ellipsoid entering water surface at an angle of attack. The obtained results are summarized and conclusion is drawn in §7.

2. Shape function of a body during its impact on the water surface

To determine the function $f(x, y, t)$ in (1.1), we consider the equations describing the position of the surface of a moving body by taking into account a possible variation of the body shape over time. Let the surface of the body be described by the equation $z_1 = F(x_1, y_1, t)$ in the coordinate system moving together with the body and such that the global x, y, z and local x_1, y_1, z_1 coordinates coincide at the impact instant $t = 0$. Here $F(0, 0, t) = 0$, $F_{,x_1}(0, 0, t) = 0$, $F_{,y_1}(0, 0, t) = 0$ and $F(x_1, y_1, t) > 0$, where $|x_1| > 0$, $|y_1| > 0$ are small. The body surface, $z_1 = F(x_1, y_1, t)$, is hence approximated close to the origin by the Taylor series

$$z_1 = \frac{x_1^2}{2R_x(t)} + \frac{y_1^2}{2R_y(t)} + O\left(\frac{r_1^4}{R^3}\right), \tag{2.1}$$

where $r_1^2 = x_1^2 + y_1^2$ and R is an averaged curvature radius. We suppose that $R_y(t) \geq R_x(t)$ and introduce $\epsilon = \sqrt{1 - R_x(t)/R_y(t)}$ as the eccentricity of the horizontal, $z_1 = \text{const.}$, sections of the elliptic paraboloid (2.1).

The body displacements in x-, y- and z-directions are given by the functions $x_b(t)$, $y_b(t)$ and $-h(t)$, respectively. The body also rotates with an angle $\alpha_x(t)$ around the x_1-axis (roll angle), $\alpha_y(t)$ around the y_1-axis (pitch angle), $\alpha_z(t)$ around the z_1-axis (yaw angle). We assume that the displacements $x_b(t), y_b(t), h(t)$ and the angles $\alpha_x(t), \alpha_y(t), \alpha_z(t)$ are small and equal to zero at $t = 0$. The penetration depth $h(t)$ is chosen here to characterize the initial stage during which $h(t)/R_x(t) \ll 1$. The orders of other displacements and angles will be specified below.

For small angles of rotation the global and local coordinates are related by the following equations:

$$x = x_1 + x_b(t) - y_1\alpha_z(t) - z_1\alpha_y(t), \tag{2.2}$$

$$y = y_1 + y_b(t) + x_1\alpha_z(t) - z_1\alpha_x(t) \tag{2.3}$$

and

$$z = z_1 - h(t) + x_1\alpha_y(t) + y_1\alpha_x(t). \tag{2.4}$$

The linear size of the wetted area is estimated by neglecting all motions except the vertical one and by neglecting the free surface elevation. Within this rough approximation, the wetted area is enclosed by the intersection line between the entering body $z = x^2/(2R_x(t)) + y^2/(2R_y(t)) - h(t)$ and the plane $z = 0$. Therefore, x and y in the wetted area are of the order of $\sqrt{h(t)R_x(t)}$ for small $h(t)/R_x(t)$. All terms in equations (2.2)–(2.4) are of the same order during the initial stage if $x_b(t)$ and $y_b(t)$ are of the order of $\sqrt{h(t)R_x(t)}$, and the angles $\alpha_x(t)$, $\alpha_y(t) = O(\sqrt{h(t)/R_x(t)})$, $\alpha_z(t) = O(1)$ as $h(t)/R_x(t) \ll 1$. Note that any yaw angles are allowed but we assume $\alpha_z(t) \ll 1$ in the next developments, keeping in mind that the duration of the initial stage is small and the yaw angle, as other angles cannot vary significantly during this short period. With these orders of the motions all terms in (2.4) are of the same order. In (2.3), all terms are of order of $O(\sqrt{h(t)R_x(t)})$ except the last term which is of a higher order, $O(\sqrt{h^3(t)/R_x(t)})$, and can be neglected in the leading order. A similar analysis applied to (2.2) finally provides that relations (2.2)–(2.4) can be approximated in the leading order by

$$x = x_1 + x_b(t), \quad y = y_1 + y_b(t), \quad z = z_1 - h(t) + x_1\alpha_y(t) + y_1\alpha_x(t). \tag{2.5}$$

Substituting (2.5) in (2.1) and rearranging the terms, we obtain

$$z = \frac{(x - X(t))^2}{2R_x(t)} + \frac{(y - Y(t))^2}{2R_y(t)} - Z(t), \tag{2.6}$$

where

$$X(t) = x_b(t) - R_x(t)\alpha_y(t), \quad Y(t) = y_b(t) - R_y(t)\alpha_x(t) \tag{2.7}$$

and

$$Z(t) = h(t) + \tfrac{1}{2}[R_y(t)\alpha_x^2(t) + R_x(t)\alpha_y^2(t)]. \tag{2.8}$$

The right-hand side in (2.6) provides the function $f(x, y, t)$ in the formulation (1.1). Note that the horizontal displacements of the body, $x_b(t)$ and $y_b(t)$, are allowed to be much greater than the vertical displacement $h(t)$.

3. Displacement potential in the contact region

The expression of the shape function $f(x, y, t)$ following from equation (2.8) makes it possible to introduce the self-similar variables λ, μ, ν as in Korobkin [7]

$$x = X(t) + B(t)\lambda, \quad y = Y(t) + B(t)\mu, \quad z = B(t)\nu, \quad B(t) = \sqrt{2R_x(t)Z(t)}, \tag{3.1}$$

and the new potential $\Phi(\lambda, \mu, \nu)$ by

$$\phi = Z(t)B(t)\Phi(\lambda, \mu, \nu). \tag{3.2}$$

The boundary-value problem with respect to the new unknown potential Φ follows from (1.1)

$$\left.\begin{aligned} &\nabla^2\Phi = 0 \quad (\nu < 0),\\ &\Phi = 0 \quad (\nu = 0,\ (\lambda, \mu) \notin D_\epsilon),\\ &\Phi_{,\nu} = \lambda^2 + (1 - \epsilon^2)\mu^2 - 1 \quad (\nu = 0,\ (\lambda, \mu) \notin D_\epsilon),\\ &\Phi \to 0 \quad (\lambda^2 + \mu^2 + \nu^2 \to \infty),\\ &\text{and} \quad \Phi \in C^2(\nu < 0) \cap C^1(\nu \le 0). \end{aligned}\right\} \tag{3.3}$$

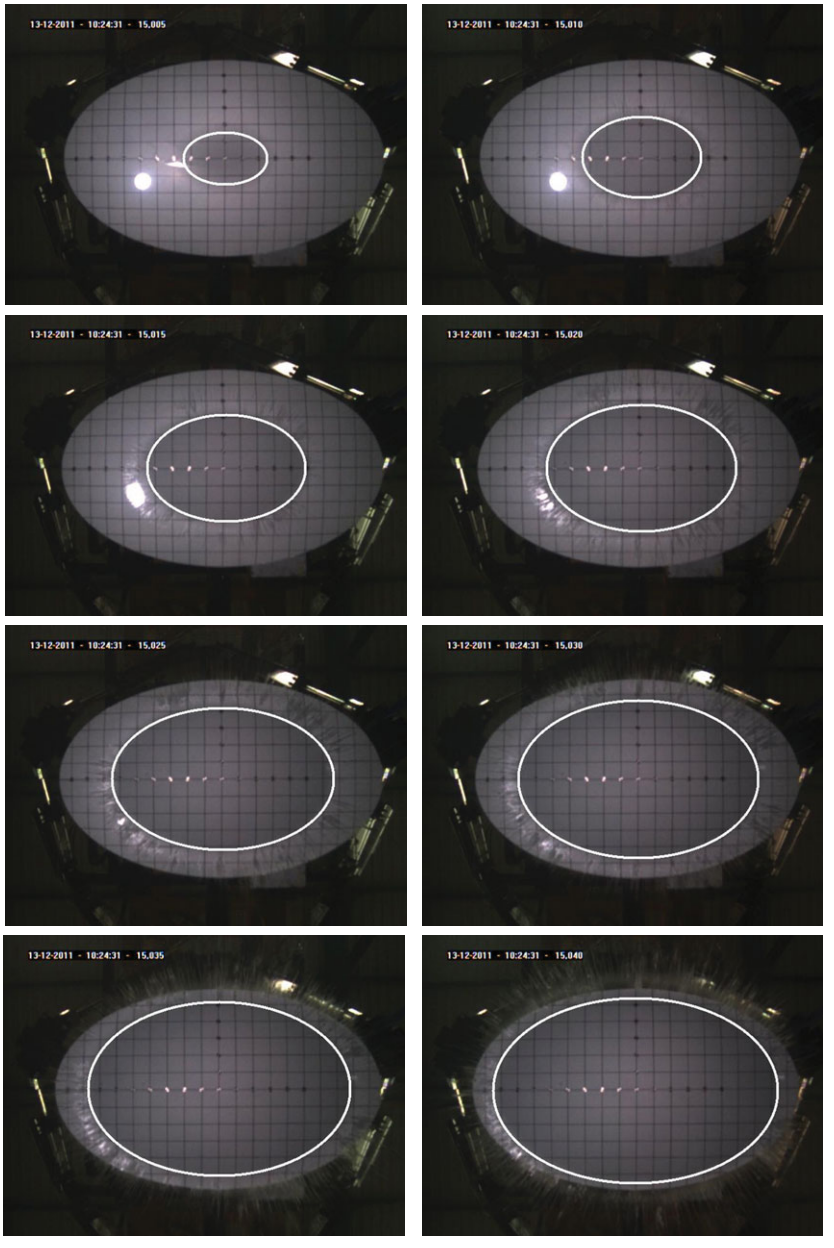

Figure 2. Snapshots of the expanding wetted surface for an oblique entry of elliptic paraboloid defined by $R_x = 0.75$ m and $R_y = 2$ m. The experimental set-up is described in Scolan [17]. The constant vertical velocity and y-horizontal velocity are $\dot{h} = 0.79\ \mathrm{m\,s^{-1}}$ and $\dot{y}_b = 0.59\ \mathrm{m\,s^{-1}}$, respectively. There are no rotations in the experiments. The camera records at 200 Hz. The periphery of the wetted area of the body surface at different time instants is marked by a thick white line. (Online version in colour.)

Here D_ϵ is the contact region in the stretched variables. Its shape depends on the only parameter $\epsilon = \sqrt{1 - R_x(t)/R_y(t)}$. The problem (3.3) is the same as that for an elliptic paraboloid entering the liquid vertically at constant speed. The solution of the latter problem was well investigated [6–8, 15] in the past. It was found that the contact region D_ϵ is the ellipse

$$\frac{\lambda^2}{a^2} + \frac{\mu^2}{b^2} \leq 1, \tag{3.4}$$

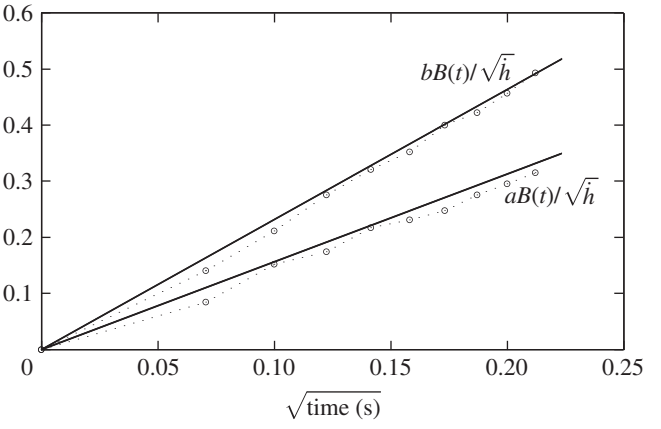

Figure 3. Time variations of the major and minor semi-axes of the elliptic wetted surface, respectively, $bB(t)$ and $aB(t)$, divided by $\sqrt{\dot{h}}$. Comparison of experimental data (dotted lines with circles) and theoretical results (solid lines). The vertical velocity and y-horizontal velocity are $\dot{h} = 0.79\ \mathrm{m\,s^{-1}}$ and $\dot{y}_b = 0.59\ \mathrm{m\,s^{-1}}$, respectively.

where $a = \sqrt{1-e^2}b$, $b = \sqrt{3/(2-e^2-\epsilon^2)}$ and $e(\epsilon)$ is the eccentricity of the contact region defined by the equation

$$\epsilon^2 = \frac{2(e^4 - e^2 + 1)E(e)/K(e) - (1-e^2)(2-e^2)}{(1+e^2)E(e)/K(e) + e^2 - 1}, \tag{3.5}$$

where $K(e)$ and $E(e)$ are the complete elliptic integrals of the first and second kind [16]. The displacement potential $\Phi(\lambda, \mu, 0)$ in the contact region is given by Korobkin [7] in the form

$$\Phi(\lambda, \mu, 0) = -\frac{2a}{3E(e)}\left(1 - \frac{\lambda^2}{a^2} - \frac{\mu^2}{b^2}\right)^{3/2}. \tag{3.6}$$

Note that the displacement potential (3.6) in the stretched coordinates system does not only depend on any motions but only on the eccentricity of the body sections. This eccentricity can be a function of time.

The comparison between theoretical and experimental results are illustrated in figures 2 and 3. We consider the oblique entry of an elliptic paraboloid defined by the constant curvature radii $R_x = 0.75\,\mathrm{m}$ and $R_y = 2\,\mathrm{m}$. The kinematics of the moving (undeformable) body reduce to two translational motions in the plane (y, z). The y-horizontal and vertical velocities are $\dot{y}_b = 0.59\ \mathrm{m\,s^{-1}}$ and $\dot{h} = 0.79\ \mathrm{m\,s^{-1}}$, respectively. The expansion of the wetted surface is computed and compared to the observations made during an experimental programme at BGO First (La Seyne/Mer, France) in 2011. This programme is described in Scolan [17]. A submerged camera is placed on the basin floor below the impact point. It records along a vertical axis upwards at a frequency of 200 frames per second. In figure 2, the periphery of the wetted surface at different time instants is marked by a thick white line. Indeed, this line is elliptic and it is not affected by the horizontal motion. The results are collected in figure 3. Since the velocities are constant, it is expected that the lengths of the wetted surface increase as $\sqrt{t}$, hence the quantities $aB/\sqrt{\dot{h}}$ and $bB/\sqrt{\dot{h}}$ are plotted in terms of $\sqrt{t}$. The variation is therefore linear. The agreement is satisfactory as the error between experiments and theory is within 10%, even at the initial stage where it is more difficult to detect the contact line accurately. The absolute error Δa of measurement is approximately one-third the size of the cell grid (0.05 m) yielding the highest relative error of 20%. More results are available in Scolan & Korobkin [18]. In particular, it is observed that the theory slightly overpredicts the experimental data regarding the size of the wetted surface.

4. Hydrodynamic loads and equations of the body motions

Taking into account that the hydrodynamic pressure p, the velocity potential φ and the displacement potential ϕ as well, are zero on the free surface and at infinity, the expressions of the force $\boldsymbol{F}$ and moment $\boldsymbol{M}$ can reduce to

$$\boldsymbol{F}(t) = \frac{\mathrm{d}}{\mathrm{d}t}\int\int_{\tilde{D}(t)} \rho\varphi \boldsymbol{n}\,\mathrm{d}S, \quad \boldsymbol{M}(t) = \frac{\mathrm{d}}{\mathrm{d}t}\int\int_{\tilde{D}(t)} \rho\varphi(\boldsymbol{r}\times\boldsymbol{n})\,\mathrm{d}S, \tag{4.1}$$

as shown in Kochin [19] for a body moving in unbounded fluid (see pp. 394–397). Here ρ is the density of the liquid. The hydrodynamic moment $\boldsymbol{M}_1(t)$ with respect to the point of the first contact on the body surface, $\boldsymbol{r}_b(t) = (x_b, y_b, -h)$, is calculated as

$$\boldsymbol{M}_1(t) = \boldsymbol{M}(t) - \boldsymbol{r}_b(t)\times\boldsymbol{F}(t), \tag{4.2}$$

If the position of the entering body is given by the equation $z = f(x, y, t)$ as in (1.1), then

$$\boldsymbol{r} = (x, y, f(x, y, t)), \quad \boldsymbol{n}\,\mathrm{d}S = (f_{,x}, f_{,y}, -1)\,\mathrm{d}x\,\mathrm{d}y. \tag{4.3}$$

The shape function $f(x, y, t)$ is given by (2.6) and the displacement potential ϕ by (3.2) and (3.6). It should be noted that $ff_{,x}, ff_{,y} = O(h\sqrt{h/R_x})$ and $x, y = O(\sqrt{hR_x})$. Therefore, the terms $ff_{,x}$ and $ff_{,y}$ can be neglected with the relative accuracy $O(h/R_x)$. The vertical component of the moment is smaller than two other components and the hydrodynamic loads do not depend on the small yaw angle $\alpha_z(t)$. Therefore, the yaw motion can be computed by integration of the corresponding equation, in which the moment is independent of this angle, after other motions have been determined. The equation for the yaw angle is not considered in the following.

Evaluating the integrals in (4.1), we obtain

$$F_x(t) = -\frac{\mathrm{d}}{\mathrm{d}t}\left(\frac{\rho A(t)}{R_x(t)}\frac{\mathrm{d}X}{\mathrm{d}t}\right), \quad F_y(t) = -\frac{\mathrm{d}}{\mathrm{d}t}\left(\frac{\rho A(t)}{R_y(t)}\frac{\mathrm{d}Y}{\mathrm{d}t}\right), \quad F_z(t) = \frac{\mathrm{d}^2}{\mathrm{d}t^2}(\rho A(t)), \tag{4.4}$$

$$M_x(t) = \frac{\mathrm{d}^2}{\mathrm{d}t^2}(\rho A(t)Y(t)), \quad M_y(t) = -\frac{\mathrm{d}^2}{\mathrm{d}t^2}(\rho A(t)X(t)) \tag{4.5}$$

and

$$A(t) = -\int\int_{D(t)} \phi(x, y, 0, t)\,\mathrm{d}x\,\mathrm{d}y = N(\epsilon)Z^{5/2}(t)R_x^{3/2}, \quad N(\epsilon) = \frac{8\sqrt{2}\pi a^2 b}{15E(e)}. \tag{4.6}$$

Note that ϵ in (4.6) can be a function of time for varying radii of the body curvature. It is important to note that $F_z(t)$ is independent of the body displacements $x_b(t)$ and $y_b(t)$ in horizontal directions. However, the force and the moments are strongly dependent on the angles of the body rotations.

If the body is free to move after impact, then the equations of the body motions read

$$\frac{\mathrm{d}}{\mathrm{d}t}\left(m(t)\frac{\mathrm{d}x_b}{\mathrm{d}t}\right) = F_x(t), \quad \frac{\mathrm{d}}{\mathrm{d}t}\left(m(t)\frac{\mathrm{d}y_b}{\mathrm{d}t}\right) = F_y(t), \quad -\frac{\mathrm{d}}{\mathrm{d}t}\left(m(t)\frac{\mathrm{d}h}{\mathrm{d}t}\right) = F_z(t) \tag{4.7}$$

and

$$\frac{\mathrm{d}}{\mathrm{d}t}\left(J_x(t)\frac{\mathrm{d}\alpha_x}{\mathrm{d}t}\right) = M_{1x}(t), \quad -\frac{\mathrm{d}}{\mathrm{d}t}\left(J_y(t)\frac{\mathrm{d}\alpha_y}{\mathrm{d}t}\right) = M_{1y}(t), \tag{4.8}$$

where $m(t)$ is the mass of the body and $J_x(t)$, $J_y(t)$ are its moments of inertia, which could be functions of time if the body changes its shape over time. Equations (4.7) can be integrated once with the result

$$m(t)\frac{\mathrm{d}x_b}{\mathrm{d}t} = -\frac{\rho A(t)}{R_x(t)}\frac{\mathrm{d}X}{\mathrm{d}t} + m(0)\dot{x}_b(0), \quad m(t)\frac{\mathrm{d}y_b}{\mathrm{d}t} = -\frac{\rho A(t)}{R_y(t)}\frac{\mathrm{d}Y}{\mathrm{d}t} + m(0)\dot{y}_b(0) \tag{4.9}$$

and

$$m(t)\frac{\mathrm{d}h}{\mathrm{d}t} + \frac{\mathrm{d}(\rho A)}{\mathrm{d}t} = m(0)\dot{h}(0). \tag{4.10}$$

Here $\dot{x}_b(0)$, $\dot{y}_b(0)$ and $-\dot{h}(0)$ are the initial velocities of the body motions in x-, y- and z-directions. Equations (4.9) yield the speeds of the horizontal motions in terms of the angles of rotation, their

time derivatives and the vertical displacement $h(t)$

$$\frac{\mathrm{d}x_b}{\mathrm{d}t} = \frac{\dot{x}_b(0)m(0)/m(t) + m_x(t)[R_x\alpha_y]_{,t}}{1+m_x(t)} \quad \text{and} \quad \frac{\mathrm{d}y_b}{\mathrm{d}t} = \frac{\dot{y}_b(0)m(0)/m(t) + m_y(t)[R_y\alpha_x]_{,t}}{1+m_x(t)}, \tag{4.11}$$

where

$$m_x(t) = \frac{\rho A(t)}{m(t)R_x(t)} \quad \text{and} \quad m_y(t) = \frac{\rho A(t)}{m(t)R_y(t)}. \tag{4.12}$$

The vertical displacement $h(t)$ is governed by equation (4.10) which can be integrated in time if the mass of the body is constant. It is convenient to introduce the length scale

$$L = \left(\frac{m}{\rho N(\epsilon)}\right)^{2/3} \frac{1}{R_x(t)}, \tag{4.13}$$

and a new non-dimensional displacement $\tilde{Z} = Z(t)/L$. Then equation (4.10) provides

$$\tilde{Z} + \tilde{Z}^{5/2} = \frac{\dot{h}(0)t}{L} + \frac{R_y(t)}{2L}\alpha_x^2 + \frac{R_x(t)}{2L}\alpha_y^2. \tag{4.14}$$

The nonlinear equation (4.14) serves to calculate $\tilde{Z}(t)$ for given angles of rotation $\alpha_x(t)$ and $\alpha_y(t)$ at time t. Note that we did not use equations for the radii of the body curvature. We assume below that the $R_x(t)$ and $R_y(t)$ are given functions of time.

An application is described in the electronic supplementary material. Given the time variations of the seven variables $(h, R_x, R_y, \alpha_x, \alpha_y, x_b, y_b)$ (hence denoted 7 d.f. case) which completely define the state of the dynamical system, the expansion of the wetted surface and the time variation of the loads are assessed. The influence of complex kinematics on the loads is also examined for a free drop configuration; in that case the 7 d.f. and the 1 d.f. case (pure vertical motion) are compared.

5. Pressure distribution

The pressure follows from the linearized Bernoulli equation $p = -\rho\varphi_{,t} = -\rho\phi_{,t^2}$, where $\phi(x, y, 0, t)$ in the wetted area is given by (3.1), (3.2) and (3.6). If we note $\phi = -G^{3/2}(x, y, t)$, then G appears as a polynomial of order 2 with respect to x and y and we can express G as

$$G(x, y, t) = \sum_{i,j=0}^{i+j\leq 2} \beta_{ij}(t)x^i y^j, \tag{5.1}$$

where all (non-zero) coefficients β_{ij} only depend on time. Then the pressure can be expressed as

$$p = \frac{3\rho}{4\sqrt{G}}(2\ddot{G}G + \dot{G}^2), \tag{5.2}$$

where overdot stands for time derivative and the expression $2\ddot{G}G + \dot{G}^2$ is a polynomial of order 4 in x and y.

We first examine the behaviour of the pressure close to the contact line, where $G(x, y, t)$ vanishes and the pressure is approximated by

$$p(x, y, 0, t) \approx \frac{3}{4}\rho \frac{C^{3/2}}{\sqrt{1-\lambda^2/a^2-\mu^2/b^2}} \left(\frac{\partial}{\partial t}\left(\frac{\lambda^2}{a^2} + \frac{\mu^2}{b^2}\right)\right)^2. \tag{5.3}$$

The time derivative in (5.3) is calculated for fixed x and y by taking into account the relations (3.1) between x, y and λ, μ. As also noted by Moore *et al.* [10], this time derivative is proportional to the normal velocity of expansion of the wetted surface and the first time instant $t^\star$, when this derivative is zero, provides the duration of the Wagner stage of impact. To find $t^\star$ and the place on the expanding contact line, where the derivative is zero at $t^\star$, we search the minimum of the

time derivative in (5.3). After some manipulations, and assuming that the ratio $R_x(t)/R_y(t)$ does not depend on time, it is shown that $t^\star$ is obtained from

$$a^2\dot{B}^2(t^\star) = \dot{X}^2(t^\star) + k^2\dot{Y}^2(t^\star). \tag{5.4}$$

The above equation provides the duration of the Wagner stage $t^\star$ for a body whose aspect ratio $k_\gamma = \sqrt{R_x/R_y}$ is constant and which moves with 5 d.f. Note that the yaw motion can be approximately neglected during the early stage of impact. Under the same assumptions, it is also shown that the pressure vanishes in the direction of the translational motion. The calculations are more complicated for a general case, where k_γ is a function of time.

We are concerned in the following with the zones of negative pressure in the contact region. These zones are bounded by the lines $p(x, y, 0, t) = 0$, which are defined by the equation $\dot{G}^2 + 2\ddot{G}G = 0$ as follows from (5.2). In the latter equation, the first term is positive and $G(x, y, t) \geq 0$ in the contact region. Therefore, the negative pressure zone may exist only if $\ddot{G}(x, y, t) \leq 0$. Then it would be of interest to determine the roots of the polynomial $\dot{G}^2 + 2\ddot{G}G$. In practice it is not an easy task to find the lines $p = 0$. On the other hand, provided that the time variations of $(h, R_x, R_y, \alpha_x, \alpha_y, x_b, y_b)$ are given, the numerical computations of the coefficients β_{ij} and their first and second derivatives in time are rather straightforward. For example, a finite difference scheme is expected to be accurate enough to compute $\dot{\beta}_{ij}$ and $\ddot{\beta}_{ij}$ if the time variations of $(h, R_x, R_y, \alpha_x, \alpha_y, x_b, y_b)$ are regular.

The pressure distribution on the wetted surface is studied below for a rigid three-dimensional body with constant radii of curvature R_x and R_y. In this case, the identity holds: $2Z\dot{B} = \dot{Z}B$ at any time, and $\dot{G}$ calculated from (5.1) does not contain polynomials of x and y greater than 1. By introducing the change of variables between coordinates systems (λ, μ) and (ξ, η) as follows:

$$\xi(x, y, t) = \frac{\sqrt{2}}{a}\left(\frac{a^2\dot{B}}{2} + \lambda\dot{X} + k^2\mu\dot{Y}\right), \quad \eta(x, y, t) = \frac{1}{b}(\mu\dot{X} - \lambda\dot{Y}), \tag{5.5}$$

we can rearrange $2\ddot{G}G + \dot{G}^2$ in equation (5.2), so that

$$\frac{4p\sqrt{G}}{3\rho H^2} = 2Z\left(1 - \frac{\lambda^2}{a^2} - \frac{\mu^2}{b^2}\right)G^{(2)} + \frac{4Z^2}{a^2B^2}\left(\frac{a^2\dot{B}^2}{2} - \dot{X}^2 - k^2\dot{Y}^2 + \xi^2 + \eta^2\right), \tag{5.6}$$

with

$$G^{(2)} = \left(\frac{a\sqrt{8R_x}}{3E}\right)^{2/3}\left(\ddot{Z} + \frac{2Z}{B}\left(\frac{\lambda\ddot{X}}{a^2} + \frac{\mu\ddot{Y}}{b^2}\right)\right). \tag{5.7}$$

We can conclude that the second term in (5.6) is positive in the contact region $D(t)$ as long as

$$T(t) = \frac{a^2\dot{B}^2}{2} - \dot{X}^2 - k^2\dot{Y}^2 > 0. \tag{5.8}$$

The above criterion is quite in line with the results of Moore *et al.* [10] who also dealt with the oblique entry of an elliptic paraboloid. As soon as the left-hand side of equation (5.8) changes its sign, and provided the body motion is such that $G^{(2)} = 0$, the pressure becomes negative in a region which is circular in variables (ξ, η) and starts to increase from $\xi = 0$ and $\eta = 0$. The location of the first point (x_o, y_o) in the contact region where $p \leq 0$, and the time instant of its appearance t_o are defined by $\xi(x_o, y_o, t_o) = 0$ and $\eta(x_o, y_o, t_o) = 0$, with

$$x_o = X - \frac{\dot{X}a^2B\dot{B}}{2(\dot{X}^2 + k^2\dot{Y}^2)} \quad \text{and} \quad y_o = Y - \frac{\dot{Y}a^2B\dot{B}}{2(\dot{X}^2 + k^2\dot{Y}^2)}, \tag{5.9}$$

where all quantities are evaluated at time t_o. Once it happens, the wetted surface where the pressure is negative increases monotonically. The corresponding surface is a circle in the coordinate system (ξ, η). In the coordinate system (x, y), that area is constructed parametrically

by inverting the linear system (5.5) with $\xi = rT(t)\cos\gamma$ and $\eta = rT(t)\sin\gamma$, where $r \in [0,1]$ and $\gamma \in [0, 2\pi]$.

As an example, we restrict the body kinematics to translational motions in the plane (y,z) with $\dot{X} = 0$. By introducing the non-dimensional measure of time $\tau = \dot{Y}/b\dot{B}$, the instant at which the pressure first vanishes in the contact region corresponds to $\tau = 1/\sqrt{2}$ as it follows from equation (5.8). The expanding elliptic area of negative pressure is enclosed by the curve

$$\frac{x^2}{a^2B^2} + 2\frac{(y - Y + bB/2\tau)^2}{b^2B^2} = 1 - \frac{1}{2\tau^2}. \tag{5.10}$$

The above ellipse is centred at a point $x_e = 0$ and $y_e = Y - bB/2\tau$, in the downstream part of the wetted surface with respect to the y translational motion. The aspect ratio of this ellipse is $\sqrt{2}k$ and can be greater than 1 if $R_x/R_y > 0.42$. Note that the aspect ratio of the contact region (3.4) is equal to k. The time $t^\star$ at which the negative pressure zone (5.10) approaches the contact line (3.4) corresponds to $\tau = 1$, i.e. when the translational velocity $\dot{Y}$ becomes equal to the velocity of expansion of the wetted surface $b\dot{B}$. The corresponding point of intersection is $x_i = 0$ and $y_i = Y - bB$. The negative pressure area hence extends over half the wetted surface, downstream. At the point of intersection, the radii of curvature (in the horizontal plane) of the two curves, the contact line and the zero pressure line (equation (5.10)) are identical bBk^2. Therefore, the two curves do not intersect elsewhere than at point (x_i, y_i).

In the electronic supplementary material, the evolution of the negative pressure zone is assessed for a more general case. It is shown that the negative pressure surface may expand much faster than the wetted surface itself.

6. Oblique impact of an ellipsoid on the flat-free surface

This section is motivated by the problem of aircraft landing on the water surface. The fuselage of an aircraft is an elongated structure and hydrodynamic loads acting on it during landing can be described by the strip theory [3]. By 'strip theory' we mean a way to construct a three-dimensional flow solution over an elongated body by computing successive two-dimensional solutions in cross sections perpendicular to the direction of the maximum elongation of a body. However, at the very beginning of the landing, the contact region of the fuselage is not elongated and the three-dimensional impact theory should be used to describe the loads during this stage.

As an illustration we consider the oblique impact of the ellipsoid

$$\frac{\hat{x}^2}{\hat{a}^2} + \frac{\hat{y}^2}{\hat{b}^2} + \frac{\hat{z}^2}{\hat{c}^2} = 1 \tag{6.1}$$

on an initially flat water surface $z = 0$. In equation (6.1), $\hat{x}$, $\hat{y}$ and $\hat{z}$ are local coordinates with the origin at the centre of the ellipsoid, and $\hat{a}$, $\hat{b}$ and $\hat{c}$ are the corresponding semi-axis. Initially, the ellipsoid is above the flat-free surface, inclined at an angle α_0 and touches the free surface at the origin of the global coordinate system x, y, z. Then the body starts to move in the (x,z) plane with the global coordinates of its centre being $x_c(t)$ and $z_c(t)$ and the angle of rotation $\alpha(t)$, where $\alpha(0) = \alpha_0$ and

$$z_c(0) = \sqrt{\hat{c}^2\cos^2\alpha_0 + \hat{a}^2\sin^2\alpha_0} \quad \text{and} \quad x_c(0) = \frac{(\hat{a}^2 - \hat{c}^2)\sin\alpha_0\cos\alpha_0}{z_c(0)}. \tag{6.2}$$

In this section, the displacements $X_c(t) = x_c(t) - x_c(0)$ and $Z_c(t) = z_c(t) - z_c(0)$, and the angle $\alpha(t)$ are assumed to be given functions of time t. Using the relations

$$\hat{x} = (x - x_c)\cos\alpha + (z - z_c)\sin\alpha, \quad \hat{z} = -(x - x_c)\sin\alpha + (z - z_c)\cos\alpha, \quad \hat{y} = y \tag{6.3}$$

between the local and global coordinates, equation (6.1) can be written in the global coordinates and approximated around the point of the first contact, $x = y = z = 0$, in a similar way as it has

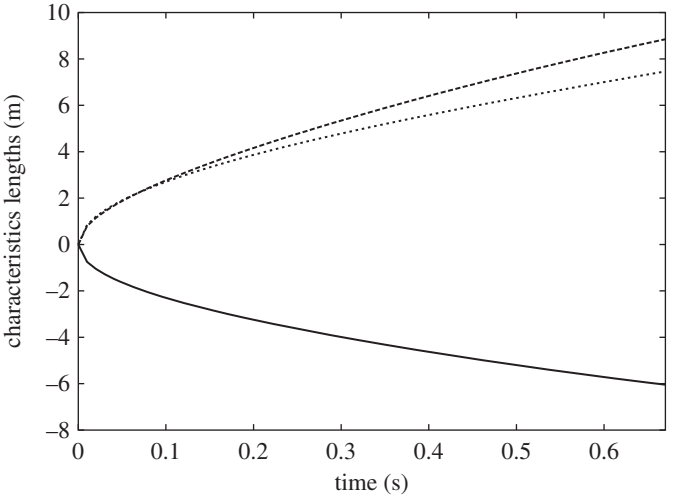

Figure 4. Time variations of positions of three points of the contact line: front point x_p (dashed line), rear point x_m (solid line) and lateral point y_p (dotted line).

been done in §2 (see equation (2.6)). The difference is that now the body motion is described with respect to its centre and the angle of the body rotation is not assumed to be small. The result is

$$z \approx \frac{(x - X(t))^2}{2R_x(t)} + \frac{y^2}{2R_y(t)} - Z(t), \tag{6.4}$$

where

$$R_x(t) = \hat{A}^3(t)\hat{D}^3(t)\hat{a}^2\hat{c}^2, \quad R_y(t) = \hat{A}(t)\hat{D}(t)\hat{b}^2, \quad X(t) = R_x^2(t)K(t), \tag{6.5}$$

$$Z(t) = R_x(t)K^2(t) + \frac{\hat{D}(t)}{\hat{A}(t)} - \frac{x_c(t)\hat{B}(t)}{\hat{A}^2(t)} - z_c(t) \tag{6.6}$$

and

$$\hat{A}(t) = \sqrt{\hat{a}^{-2}\sin^2\alpha(t) + \hat{c}^{-2}\cos^2\alpha(t)}, \quad \hat{B}(t) = (\hat{a}^{-2} - \hat{c}^{-2})\sin\alpha(t)\cos\alpha(t), \tag{6.7}$$

$$\hat{D}(t) = \sqrt{1 - \frac{x_c^2(t)}{(\hat{A}\hat{a}\hat{c})^2}}, \quad K(t) = \frac{\hat{B}(t)}{\hat{A}^2(t)} + \frac{x_c(t)}{(\hat{A}^3\hat{D}\hat{a}^2\hat{c}^2)}. \tag{6.8}$$

Calculations are performed for the ellipsoid with semi-axis $\hat{a} = 10\,\mathrm{m}$, $\hat{b} = 10\,\mathrm{m}$ and $\hat{c} = 3\,\mathrm{m}$, which is initially inclined at angle $\alpha_0 = -6^o$. The ellipsoid moves with the horizontal speed $5\,\mathrm{m\,s^{-1}}$ and penetrates water at speed $1\,\mathrm{m\,s^{-1}}$. The ellipsoid rotates with a constant angular velocity $\alpha(t) = \alpha_0 + \alpha_v t/T$, where $\alpha_v = 6^0$ and T is chosen as 1 s. These kinematics are arbitrary but satisfy the basic assumptions of the model.

The positions of three points of the contact line, $x_m(t)$, $x_p(t)$ and $y_p(t)$, in the global coordinates are shown in figure 4. Here $x_m(t)$ and $x_p(t)$ are the maximum and minimum x-coordinates of the contact line, and $y_p(t)$ is the y-semi-axis of the contact line. It is observed that the speed of the rear point of the contact line $\dot{x}_m(t)$ is zero at $t = 0.67\,\mathrm{s}$, which is the duration of the Wagner stage of impact in the case under consideration (see §5).

Equations (4.4)–(4.6), (6.5) and (6.6) provide the forces $F_x(t)$, $F_z(t)$ and the moment $M_c(t) = z_c F_x - x_c F_z - M_y(t)$ with respect to the centre of the ellipsoid (figure 5) during the Wagner stage, $0 < t < 0.67\,\mathrm{s}$. The vertical force $F_z(t)$ is always positive and almost linear. The horizontal force $F_x(t)$ is negative and much greater than the vertical force at the end of the Wagner stage. The moment $M_c(t)$ is positive for $0 < t < 0.3\,\mathrm{s}$ while trying to increase the angle of the ellipsoid inclination, and negative after $t > 0.3\,\mathrm{s}$ while trying to sink the ellipsoid. In these calculations, the motions of the body are prescribed.

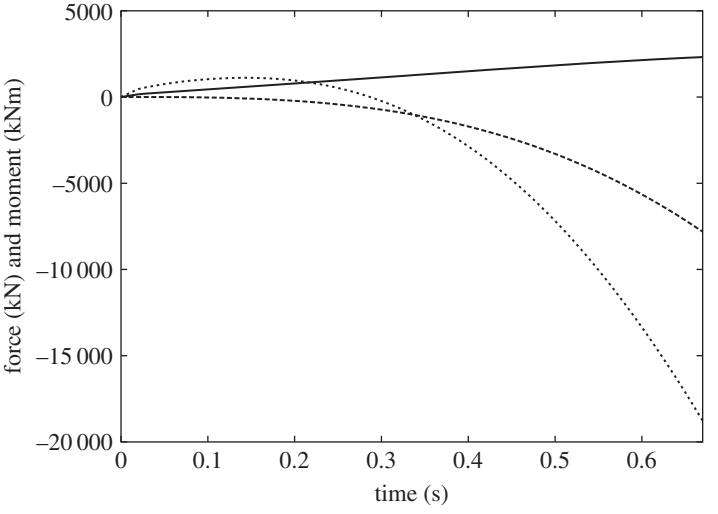

Figure 5. Time variations of the force and moment acting on the ellipsoid. Vertical force F_z (solid line), horizontal force F_x (dashed line) and pitch moment M_y (dotted line).

7. Conclusion

Three-dimensional problem of water impact by a smooth body has been studied. The body moves in 6 d.f. and changes its shape over time. The liquid flow and the pressure distribution caused by the impact were obtained within the Wagner theory of water impact. Hydrodynamic forces and moments acting on the body were derived in analytical form.

It was shown that water entry of a three-dimensional body moving with 6 d.f. is rather different from pure vertical entry of the same body. Horizontal displacements of the body and its angular motions may lead to the appearance of low-pressure zones in the wetted part of the body surface. These zones may expand in time and approach the periphery of the wetted area, which leads to separation of the liquid surface from the surface of the body at the end of the impact stage of the entry. The present Wagner model fails when cavitation effects appear and when a zone of negative pressure arrives at the contact line. The horizontal velocity of the body can be much higher than its vertical velocity within this analysis.

The ditching of an aircraft is a particular application of the present theoretical study. The ditching involves mainly the heave, surge and pitch motions of the aircraft. It was shown that the actual shape of the aircraft fuselage can be approximated by an elliptic paraboloid close to the initial contact point and the corresponding shape is characterized by time-varying radii of curvature. If the latter are large enough compared to the penetration depth, the Wagner theory provides reliable results in terms of the loads.

Comparisons with experimental results for an oblique entry of an elliptic paraboloid support the present theoretical results for moderate horizontal velocities. In particular, it is confirmed that an elliptic paraboloid entering an initially flat-free surface with both horizontal and vertical velocities also has an expanding wetted surface which is elliptic.

Disclaimer. Any opinions, findings and conclusions or recommendations expressed in this material are those of the authors and do not necessarily reflect the views of the Office of Naval Research.

Ethics statement. This work does not describe experiments on animals.

Data accessibility. The datasets supporting this article have been uploaded as part of the electronic supplementary material.

Funding statement. This study is part of the TULCS project which received funding from the European Community's Seventh Framework Programme under grant agreement no. FP7-234146. The experimental programme is partly founded by Conseil Général du Var (France). A.K. acknowledges also the support from

EC PF7 project Smart Aircraft in Emergency Situations under the grant agreement no. FP7-266172. A.K. is also grateful for the support by the NICOP research grant 'Fundamental Analysis of the Water Exit Problem' N62909-13-1-N274, through Dr Woei-Min Lin.

Author contributions. The theoretical and experimental results shown in this paper were obtained by both authors.

Conflict of interests. We have no competing interests.

References

1. Kleefsman KMT, Fekken G, Veldman AEP, Iwanowski B, Buchner B. 2005 A volume-of-fluid based simulation method for wave impact problems. *J. Comput. Phys.* **206**, 363–393. (doi:10.1016/j.jcp.2004.12.007)
2. Maruzewski P, Touzé DL, Oger G, Avellan F. 2010 SPH high-performance computing simulations of rigid solids impacting the free-surface of water. *J. Hydraul. Res.* **48**, 126–134. (doi:10.1080/00221686.2010.9641253)
3. Tassin A, Piro DJ, Korobkin AA, Maki KJ, Cooker MJ. 2013 Two-dimensional water entry and exit of a body whose shape varies in time. *J. Fluids Struct.* **40**, 317–336. (doi:10.1016/j.jfluidstructs.2013.05.002)
4. Yang Q, Qiu W. 2012 Numerical simulation of water impact for 2D and 3D bodies. *Ocean Eng.* **43**, 82–89. (doi:10.1016/j.oceaneng.2012.01.008)
5. Wagner H. 1932 Über Stoss- und Gleitvergänge an der Oberfläche von Flüssigkeiten. *ZAMM* **12**, 193–215. (doi:10.1002/zamm.19320120402)
6. Scolan YM, Korobkin AA. 2001 Three-dimensional theory of water impact. Part 1. Inverse Wagner problem. *J. Fluid Mech.* **440**, 293–326. (doi:10.1017/S002211200100475X)
7. Korobkin AA. 2002 The entry of an elliptical paraboloid into a liquid at variable velocity. *J. Appl. Math. Mech.* **66**, 39–48. (doi:10.1016/S0021-8928(02)00006-0)
8. Scolan YM, Korobkin AA. 2003 Energy distribution from vertical impact of a three-dimensional solid body onto the flat free surface of an ideal fluid. *J. Fluids Struct.* **17**, 275–286. (doi:10.1016/S0889-9746(02)00118-4)
9. Korobkin AA, Scolan YM. 2006 Three-dimensional theory of water impact. Part 2. Linearized Wagner problem. *J. Fluid Mech.* **549**, 343–374. (doi:10.1017/S0022112005008049)
10. Moore MR, Howison SD, Ockendon JR, Oliver JM. 2012 Three-dimensional oblique water-entry problems at small deadrise angles. *J. Fluid Mech.* **711**, 259–280. (doi:10.1017/jfm.2012.391)
11. Scolan Y-M, Korobkin AA. 2012 Hydrodynamic impact (Wagner) problem and Galin's theorem. In *Proc. 27th IWWWFB, Copenhagen, Denmark, 23–25 April* (eds HB Bingham, RW Read, TB Christiansen), pp. 165–168, IWWWFB.
12. Korobkin AA. 1985 Initial asymptotics in the problem of blunt body entrance into liquid. PhD thesis, Lavrentyev Institute of Hydrodynamics.
13. Howison SD, Ockendon JR, Wilson SK. 1991 Incompressible water-entry problems at small deadrise angles. *J. Fluid Mech.* **222**, 215–230. (doi:10.1017/S0022112091001076)
14. Korobkin AA, Pukhnachov VV. 1988 Initial stage of water impact. *Ann. Rev. Fluid Mech.* **20**, 159–185. (doi:10.1146/annurev.fl.20.010188.001111)
15. Korobkin AA. 2005 Three-dimensional nonlinear theory of water impact. In *Proc. 18th Int. Congr. Mechanical Engineering, Ouro Preto, Minas Gerais, Brazil, November* (eds M Ziviani, SFM Almeida), pp. 1–8, Brazilian Society of Mechanical Science and Engineering.
16. Gradshteyn IS, Ryzhik IM. 1994 *Tables of integrals*, 1204 p, 5th edn.. New York, NY: Academic Press.
17. Scolan Y-M. 2012 Hydrodynamic loads during impact of a three dimensional body with an arbitrary kinematics (in french). In *Proc. 13th Journées de l'Hydrodynamique, Chatou, France, 21–23 November* (ed. M Benôit). See http://website.ec-nantes.fr/actesjh/images/13JH/13JH-actes.htm.
18. Scolan Y-M, Korobkin AA. 2012 Low pressure occurrence during hydrodynamic impact of an elliptic paraboloid entering with arbitrary kinematics. In *Proc. 2nd Int. Conf. on Violent Flows, Nantes, France, 25–27 September* (ed. D Le Touzé), pp. 1–8 Publibook.
19. Kochin NE, Kibel IA, Roze NV. 1964 *Theoretical hydromechanics*. New York, NY: Intersciences Publishers.